Received: 21 January 2020 | Revised: 7 January 2021 | Accepted: 9 January 2021 | Published on: 25 January 2021

DOI: 10.1002/joc.7008

RESEARCH ARTICLE

International Journal of Climatology RMetS

Clothing resistance and potential evapotranspiration as thermal climate indicators—The example of the Carpathian region

Ferenc Ács[1] | **Annamária Zsákai**[2] | **Erzsébet Kristóf**[1,3] | **Amanda Imola Szabó**[1] | **Johannes Feddema**[4] | **Hajnalka Breuer**[1]

[1]Department of Meteorology, Eötvös Loránd University, Budapest, Hungary

[2]Department of Human Anthropology, Eötvös Loránd University, Budapest, Hungary

[3]Faculty of Science, Excellence Center, Eötvös Loránd University, Budapest, Hungary

[4]Department of Geography, University of Victoria, Victoria, British Columbia, Canada

Correspondence
Ferenc Ács, Department of Meteorology, Eötvös Loránd University, Budapest, Hungary.
Email: acs@caesar.elte.hu

Abstract

Clothing resistance parameter r_{cl} and potential evapotranspiration (PET), a major component of Thornthwaite type climate classifications, are used as thermal climate indicators for characterizing the thermal climate of the Carpathian region. r_{cl} is simulated by a model based on clothed human body energy balance considerations. r_{cl} refers to a walking human in outdoor conditions, whose somatotype can differ. Somatotype shapes are determined by applying the Heath–Carter somatotype method. PET is estimated using only air temperature and latitude as inputs. In addition r_{cl} is linked to PET. The annual mean of r_{cl} is statistically interconnected with annual sum of PET, and the annual fluctuation of r_{cl} ($dr_{cl} = r_{cl}^{max} - r_{cl}^{min}$) with the annual fluctuation of PET (dPET = $PET^{max} - PET^{min}$). The Carpathian region's thermal climate is analysed by comparing PET results with r_{cl} model results and r_{cl} results obtained by statistical link. We showed that r_{cl} model results are strongly sensitive to human body somatotype variations. It is also shown that the spatial heterogeneity of thermal climates is the lowest in the lowlands and the highest in the mountains. The spatial heterogeneity of r_{cl} and dr_{cl} values obtained by statistical link is comparable to the spatial heterogeneity of PET, but is lower than that obtained from the r_{cl} model. Similarly to r_{cl} model results, r_{cl} results obtained by statistical link are also sensitive to human body somatotype variations. All these results suggest that statistical connections between r_{cl} and PET and dr_{cl} and dPET can be used as subunits in Thornthwaite type climate classifications to obtain human thermal climate information. Lastly, areas with the largest thermal contrast are reproduced in terms of both the annual sum of PET and the r_{cl}, which is obtained by both the model and the statistical link.

KEYWORDS

Carpathian region, clothing resistance, human body, potential evapotranspiration, somatotype, statistical link, thermal climate

1 | INTRODUCTION

The importance of clothing in human biometeorological studies has been recognized since the 1930s (e.g., Winslow *et al*., 1937; Gagge *et al*., 1938; Winslow *et al*., 1938; Gagge *et al*., 1941). In these studies role of clothing was investigated by both experimental and theoretical tools handling it as an important input variable on the human body–atmosphere interface. In the second part of the twentieth century (e.g., Auliciems and de Freitas, 1976; de Freitas, 1979) clothing was viewed and interpreted as a human 'reaction' to environmental conditions, analysed as a determinant model output. Today, the influence of clothing on biometeorological thermal regulation is typically considered in two ways: as an input parameter (e.g., Havenith *et al*., 2012) in thermo-physiological models (e.g., Fiala *et al*., 2012) or as a model output representing thermal adaptation behaviour (Lin, 2009; Potchter *et al*., 2018). In this case, r_{cl} can be used as a measure for expressing the extent to which human body heat exchange is unbalanced. When there is an excess of heat, the human body needs cooling to reach energy balance. Then r_{cl} values are negative. Note that in studies published to date negative clothing resistance values were not considered at all, they were simply equated to zero with the argument 'Since being nude is not acceptable in public, clo values ≤ 0 were set at zero' (Yan, 2005). In this study, negative clothing resistance values are also used, since they are interpretable when clothing is viewed as a thermal regulator ignoring its human behaviour dependence. Conversely, when there is a heat deficit, the human body needs warming to reach energy balance. In this case, r_{cl} values are positive. When the human body is in energy balance, it needs neither cooling nor warming sensing this state as comfortable. In this case, r_{cl} is very close or equal to zero.

Clothing resistance parameter is a complex quantity since it depends upon both human and environmental characteristics. Among human characteristics the personal, social aspects as well as the activity type are the most determinant. Activity type determines metabolic activity rate, which can vary between 40 and 600 Wm^{-2} depending on the person. Among environmental factors, it depends upon all those factors that determine the thermal state of the environment. The most important are air temperature, radiation, wind speed and air humidity. Initially (e.g., de Freitas, 1979) rough r_{cl} estimations were made using climatological air temperature and wind speed estimations and by calculating environmental radiation. Later on (e.g., Yan and Oliver, 1996) station data of air temperature, wind speed, air humidity and cloudiness were used beside the calculation of radiation for seasonal estimates of r_{cl}. In the 21st century (e.g., Yan, 2005; Robaa and Hasanean, 2007), r_{cl} is estimated by using daily or hourly air temperature, wind speed and cloudiness data calculating environmental radiation. In the studies indicated, the human considered was either standing, or performing an easy activity. There were no sensitivity analyses at all regarding dependence between r_{cl} and environmental variables. Sensitivity analysis in the subject of the interdependence between clothing resistance, metabolic activity and environmental thermal load can be found in Campbell–Norman's book (Campbell and Norman, 1998). In this treatment environmental thermal load is represented via operative temperature. Recently, Ács *et al*. (2019) investigated the sensitivity of r_{cl} to wind speed variations and to inter-person variations of metabolic heat flux density. They compared these two effects, but did not draw definite conclusions regarding the magnitude of their impacts.

Independent of human thermal comfort studies, empirical climate classification methods have also been developed over the last century. The first quantitative empirical method is constructed by Köppen (1884, 1900, 1918, 1936) and is based on biogeographic considerations. It is still the most popular method because of its simplicity (Kottek *et al*., 2006; Rubel and Kottek, 2011). Subsequently, as a criticism to Köppen's method, the Thornthwaite method (Thornthwaite, 1931, 1948) was developed strictly on physically based parameters and without any biogeographic basis. Thornthwaite (1948) introduced the notion of potential evapotranspiration, which served as a basis for his new method. The development of the new model type has evolved over time (Thornthwaite and Mather, 1955; Willmott and Feddema, 1992; Feddema, 2005). Feddema's (2005) method can currently be treated as the end-product of the Thornthwaite-type approach.

Both clothing resistance r_{cl} and potential evapotranspiration PET can be treated as thermal climate indicators. r_{cl} is used for human climate classification purposes (e.g., Auliciems and de Freitas, 1976; Yan, 2005; Robaa and Hasanean, 2007), while PET in Thornthwaite-type climate classifications. So far, there have only been a few attempts at linking empirical and human climate classification results. In these attempts only the Köppen–Geiger method outputs were related either to Physiologically Equivalent Temperature (PET; e.g., Yang and Matzarakis, 2016; Potchter *et al*., 2018) or to Universal Thermal Climate Index (e.g., Potchter *et al*., 2018), or to clothing resistance parameter (Ács *et al*., 2020). In these analyses, the results obtained by models were not statistically linked, they were only compared. PET and r_{cl} were introduced at approximately the same time (around the middle of the last century), nevertheless they have not been linked to each other to date. By linking them

Thornthwaite-type climate classification would be able to provide extra information in terms of human thermal climates, which was our main motivation. Annual mean r_{cl} is statistically interconnected with annual sum of PET and, in a similar way, the annual fluctuation of r_{cl} ($dr_{cl} = r_{cl}^{max} - r_{cl}^{min}$) with the annual fluctuation of PET (dPET = $PET^{max} - PET^{min}$).

According to the above, this study has multiple objectives: (a) to characterize the Carpathian region thermal climate in terms of annual mean of r_{cl} and annual sum of PET using an r_{cl} model and the Feddema method; (b) to statistically link annual mean of r_{cl} with annual sum of PET and annual fluctuation of r_{cl} ($dr_{cl} = r_{cl}^{max} - r_{cl}^{min}$) with the annual fluctuation of PET (dPET = $PET^{max} - PET^{min}$) and (c) to check the behaviour of the statistical models interconnecting r_{cl} and PET and dr_{cl} and dPET. The statistical relationships between r_{cl} and PET and dr_{cl} and dPET are human-dependent, therefore these relationships should be established separately for endomorphic, mesomorphic and ectomorphic humans. Note that the r_{cl} yield is characterized by both annual mean of r_{cl} and annual fluctuation of r_{cl}. Two datasets are used in this study. Climate data refer to the Carpathian region, human data to the Hungarian people. Climate data are taken from the CarpatClim dataset (Spinoni *et al*., 2015). Somatotype analysis and the calculation of human metabolic flux density is performed by using a Hungarian human dataset (Zsákai *et al*., 2015) containing data of more than 3,000 people.

The study is organized as follows. The clothing resistance model is briefly presented in Section 2.1. The somatotype classification method is described in Section 2.2. The calculation method of PET is presented in Section 2.3. The region and climatic data are introduced in Section 2.4 and human data in Section 2.5. Results are presented in Section 3; the Carpathian region's thermal climate according to PET in Section 3.1; the somatotype classification results in Section 3.2; the r_{cl} model results in Section 3.3; the results of the statistical linking in Section 3.4 and the thermal climate results obtained by regression curves connecting r_{cl} and PET and dr_{cl} and dPET in Section 3.5. A discussion of the proposed method and the results obtained can be found in Section 4. The conclusions reached are presented in Section 5.

2 | METHODS AND DATA

The clothing resistance model, the Heath-Carter somatotype classification method, the calculation method of PET and the basic meteorological and human dataset characteristics are presented below.

2.1 | The clothing resistance model

Using energy balance equations for the human skin–clothing interface and for the clothing–air environment interface, neglecting the storage effect, we can obtain the clothing resistance parameter (Ács *et al*., 2019)

$$r_{cl} = \rho \cdot c_p \cdot \frac{T_S - T_a}{M - \lambda E_{sd} - \lambda E_r - W} - r_{Hr} \cdot \left[\frac{R_{ni}}{M - \lambda E_{sd} - \lambda E_r - W} + 1 \right], \quad (1)$$

where ρ is air density ($kg \cdot m^{-3}$), c_p is specific heat at constant pressure ($Jkg^{-1} \cdot C^{-1}$), r_{Hr} is the combined resistance for expressing the thermal radiative and convective heat exchanges (sm^{-1}), T_S is skin temperature (°C), T_a is air temperature (°C), R_{ni} is isothermal net radiation flux density (Wm^{-2}), M is metabolic heat flux density (Wm^{-2}), λE_{sd} is the latent heat flux density of dry skin (Wm^{-2}), λE_r is respiratory latent heat flux density (Wm^{-2}) and W is mechanical work flux density (Wm^{-2}), which refers to the activity under consideration. r_{cl} is calculated for a walking human in outdoor conditions whose speed is 1.1 ms^{-1} (4 $km \cdot hr^{-1}$) and skin temperature is 34°C. It can also be expressed as a function of operative temperature T_o, then

$$r_{cl} = \rho \cdot c_p \cdot \frac{T_S - T_o}{M - \lambda E_{sd} - \lambda E_r - W} - r_{Hr}, \quad (2)$$

where

$$T_o = T_a + \frac{R_{ni}}{\rho \cdot c_p} \cdot r_{Hr}. \quad (3)$$

The human body is represented as simply as possible using a one-node model (Katić *et al*., 2016). M is parameterised according to Weyand *et al*. (2010),

$$M = M_b + M_w, \quad (4)$$

where M_b is the basal metabolic flux density (Wm^{-2}) (sleeping human) and M_w is the metabolic flux density (Wm^{-2}) referring to walking. There is plethora of M_b parameterisations, we used Mifflin *et al*.'s (1990) formula after the recommendation of Frankenfield *et al*. (2005). M_w is parameterised after Weyand *et al*. (2010),

$$M_w = 1.1 \cdot \frac{3.80 \cdot M_{bo} \cdot \left(\frac{L_{bo}}{100}\right)^{-0.95}}{A_{bo}}, \quad (5)$$

where M_{bo} is body mass (kg), L_{bo} is body length (cm) and A_{bo} is body surface (m^2). A_{bo} is estimated after the well-known Dubois and Dubois (1915) formula,

$$A_{bo}=0.2\cdot M_{bo}^{0.425}\cdot\left(\frac{L_{bo}}{100}\right)^{0.725}. \quad (6)$$

M can vary from human to human, or from human group to human group depending on somatotype. Latent heat and mechanical work flux densities can be simply parameterised via M according to Campbell and Norman (1998) and Auliciems and Kalma (1979), respectively.

Air temperature and isothermal net radiation flux density are the most important environmental variables. r_{Hr} is a resistance parameter combining thermal radiative and convective heat exchange effects. It depends upon T_a and wind velocity (Campbell and Norman, 1998). In this study, r_{cl} is used as a human thermal climate indicator expressing thermal load, accordingly in the case of a heat deficit it is positive, and conversely, in the case of heat excess it is negative. In the case of thermal neutrality or comfort, it is zero or close to zero.

2.2 | The Heath–Carter somatotype classification method

Metabolic heat flux density can be linked to somatotype independent of ethnic group. This motivated us to use a somatotype method for characterizing people. Today, the Heath–Carter somatotype classification method (Carter and Heath, 1990) is the most frequently used morphological body shape categorisation method. The method uses body height, body weight, long bone widths of the extremities, circumferences on the extremities, as well as skinfold thickness both on the torso and the extremities. The output of the method is somatotype, which may be characterized by its endomorphy, mesomorphy and ectomorphy.

Endomorphy represents relative fatness. Higher ratings in this somatotype component mean larger deposits of subcutaneous fat, and so a more rounded body can be estimated. Mesomorphy is a rating on a continuum of musculo-skeletal robustness relative to stature. Higher ratings in mesomorphy mean greater muscle mass with wider bone diameters relative to stature. Ectomorphy is the component of somatotype that estimates the relative linearity or slenderness of a physique. Higher ectomorphy ratings mean a smaller body mass relative to stature and more elongated limb segments (Carter and Heath, 1990). Quantitative determinations of endomorphy, mesomorphy and ectomorphy can be found, for instance, in the work of Bodzsár and Zsákai (2004).

The individual somatotypes were estimated by using the following regression equations introduced by Carter *et al.* (1983):

$$ENM=-0.7182+0.1451\cdot S-0.00068\cdot S^2+0.0000014\cdot S^3, \quad (7)$$

$$MEM=0.858\cdot HB+0.601\cdot FB+0.188\cdot AC+0.161\cdot CC-0.131\cdot He+4.5, \quad (8)$$

$$ECM=\begin{cases}0.732\cdot HWR-28.58, & \text{if } HWR\geq 40.75\\ 0.463\cdot HWR-17.63, & \text{if } 38.25<HWR<40.75\\ 0.1, & \text{if } HWR\leq 38.25,\end{cases} \quad (9)$$

where ENM is endomorphy, MEM is mesomorphy, ECM is ectomorphy S is the sum of the triceps, subscapular and supraspinal skinfolds (mm), HB is humerus biepicodylar width (cm), FB is femur biepicodylar width (cm), AC is upper arm circumference (cm, corrected with skinfold thickness on the triceps), CC is calf circumference (cm, corrected with skinfold thickness on the calf), He is height (cm) and HWR is ponderal index. HWR is calculated as

$$HWR=\frac{\text{height (cm)}}{\text{weight (kg)}^{1/3}}. \quad (10)$$

2.3 | Calculation of PET

There are many formulae (e.g., Jianbiao *et al.*, 2005) for estimating PET, the simplest PET formulae use only air temperature T_a and latitude as inputs (e.g., Xu and Singh, 2001). We used the Thornthwaite type (1948) formula based on T_a and daylight length, as presented in McKenney and Rosenberg (1993). For the i^{th} month ($i = 1, ...,12$)

$$PET_i=1.6\cdot\left(\frac{L_i}{12}\right)\cdot\left(\frac{N_i}{30}\right)\cdot\left(\frac{10\cdot T_{ai}}{I}\right)^A, \quad (11)$$

where I is a heat index introduced by Thornthwaite (1948) as

$$I=\sum_{i=1}^{12}t_i, \quad (12)$$

TABLE 1 The thermal types used in Feddema (2005) method

Thermal types	Annual sum of potential evapotranspiration (PET) (mm·year^{-1})
Torrid	>1,500
Hot	1,200 < PET ≤ 1,500
Warm	900 < PET ≤ 1,200
Cool	600 < PET ≤ 900
Cold	300 < PET ≤ 600
Frost	0 < PET ≤ 300

$$t_i = \begin{cases} \left(\frac{T_{ai}}{5}\right)^{1.514}, & \text{if } T_{ai} > 0 \\ 0, & \text{if } T_{ai} \leq 0 \end{cases} \quad (13)$$

$$A = 6.75 \cdot 10^{-7} \cdot I^3 - 7.71 \cdot 10^{-5} \cdot I^2 + 1.792 \cdot 10^{-2} \cdot I + 0.49239. \quad (14)$$

N_i is the number of days in the i^{th} month, T_{ai} is mean monthly air temperature (°C) of the i^{th} month and L_i is mean monthly daylight length (hr). In our calculations, L_i is estimated by calculating L_i for the central day in the month (except February the 15th day in the month) as follows,

$$L_i = \frac{24}{180} \cdot \arccos[-tg(\varphi) \cdot tg(\delta_i)], \quad (15)$$

where φ is latitude ($^\circ$) and δ_i is declination ($^\circ$) on the central day of the i^{th} month.

PET together with precipitation are the main quantities of the Feddema (2005) method. The Feddema method is a revised Thornthwaite type (Thornthwaite, 1948) method. It is strictly physically based without possessing any biogeographic basis as, for instance, in the Köppen (1918, 1936) method. It calculates and classifies heat and water availability while trying to be as simple as possible. The thermal types used in Feddema (2005) method are presented in Table 1.

Note that these thermal types are not constructed according to human thermal sensation votes; only by proportionate subdividing the range of PET.

2.4 | Region and climatic data

Climatic data are taken from the CarpatClim dataset (Spinoni *et al*., 2015). This dataset is a new product of the Hungarian Meteorological Service created in cooperation with surrounding central European services. The data chosen refer to the period 1971–2000; their spatio-temporal resolution is 0.1° × 0.1° with a daily time-step. CarpatClim data are quality controlled and homogenized daily data obtained by using MASH (Multiple Analysis of Series for Homogenization) technique. The original MASH procedure (Szentimrey, 1999) treated monthly time series, whilst its last version (MASHv3.03; Szentimrey, 2011) deals with daily series as well. It is an efficient multiple breakpoint detection method giving homogenized time series as end result (e.g., Rasol *et al*., 2008; Zhen and Zhong-Wei, 2009; Domonkos, 2013; Li *et al*., 2016; Yimer *et al*., 2021). In the MASH method relative homogeneity test procedure is applied by using additive (e.g., temperature) or multiplicative (e.g., wind) model depending on climate element considered. The method consists of two parts. In the first part, monthly data are treated (quality control, completion of missing data, homogenization of monthly series with or without using metadata providing homogenized monthly, seasonal and annual series, verification of the homogenization results), in the second part, daily data are handled (quality control, completion of missing data, homogenization of daily series by using detected monthly inhomogeneities and control of the homogenized daily series). Note that in construction of CarpatClim dataset metadata were not used. A Carpathian region climate analysis on the basis of the CarpatClim dataset can be read, for instance, in the works of Spinoni *et al*. (2012; 2015), Cheval *et al*. (2014). The CarpatClim dataset region together with the main geographical designations are presented in Figure 1.

The region is located between the 17 and 27°E longitude lines and 44–50°N latitude lines containing 6,161 grid points representing the Carpathian Basin region almost completely. In this study, we used data on global radiation, cloud cover, air temperature, vapour pressure and 10 m wind speed. Monthly data are calculated from the daily data; 30-year mean is calculated for the period 1971–2000.

2.5 | Human data

Human body characteristics are taken from a Hungarian human dataset (Utczás *et al*., 2015; Zsákai *et al*., 2015; Bodzsár *et al*., 2016) constructed at the Department of Biological Anthropology, Eötvös Loránd University, Budapest, Hungary. The dataset contains the data of about 2,000 Hungarian children and 1,000 Hungarian adults. Determination of somatotype is carried out for almost all children and adults. From this set of adults, we chose two persons who were extremely endomorphic and mesomorphic and one person who was ectomorphic. The basic human characteristics of these persons are presented in Table 2.

The most important human state variable is body mass. The humans are chosen according to their body mass regardless of their sex. We assume that there is relationship between body shape and metabolic rate. Note that for a walking human the total energy flux density M increases from ectomorphic M^{ecto} through mesomorphic M^{meso} to endomorphic M^{endo} somatotype, that is $M^{ecto} < M^{meso} < M^{endo}$.

3 | RESULTS

To give a complete analysis we will separately discuss (a) the area distribution of the annual sum of the PET values obtained by the Thornthwaite type (1948) formula, (b) the Heath–Carter somatotype classification method results, (c) the area distribution characteristics of r_{cl} fields obtained from the r_{cl} model, (d) the main characteristics of the regression curves obtained by linking r_{cl} and PET and dr_{cl} and dPET values and (e) the area distribution characteristics of the r_{cl} fields obtained by using regression curves. r_{cl} related discussions are performed for persons whose somatotypes are very different.

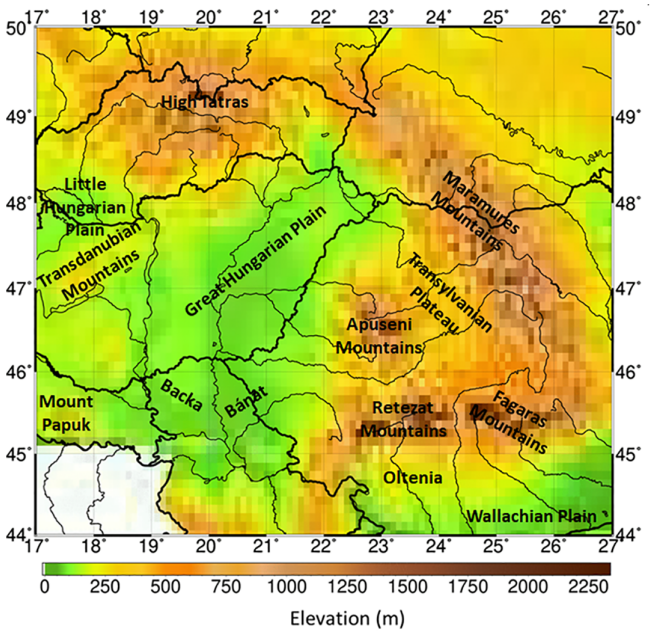

FIGURE 1 The CarpatClim dataset region with basic elevation data and the major geographical designations used in the study [Colour figure can be viewed at wileyonlinelibrary.com]

3.1 | The thermal climate of the Carpathian region according to PET

The area distribution of the annual sum of PET in the Carpathian region for the period 1971–2000 is presented in Figure 2.

According to Thornthwaite (1948) or Feddema (2005) two thermal types can be distinguished; the thermal type 'cold' (blue on the map) in the mountains (concretely Mount Papuk, the Apuseni Mountains, the Carpathians) and the thermal type 'cool' (orange and red) in the lower regions (the Little Hungarian Plain, the Great Hungarian Plain, the Wallachian Plain and Bačka and Banat). In lower parts of Ukraine, as well as in many areas of the Transylvanian Plateau an intermediate thermal type 'cold/cool' (green) is observable. Note that the Thornthwaite/Feddema methods do not treat annual fluctuation of PET.

3.2 | Heath-Carter somatotype classification results

The morphological body shape of the three studied subjects can be summarized as follows (Table 3): the endomorphic component (9.24) dominates (the component is greater by at least 1 component unit than the other components) in the endomorphic female's somatotype, her relative fatness is rather high, however the mesomorphic component (7.42) is high as well, so her body shape is characterized by robust musculo-skeletal development, too. The mesomorphic male's somatotype is also characterized by an increased level of musculo-skeletal robusticity and fatness, but in his case the mesomorhic component (8.80) is dominant. In the case of the ectomorphic female these two components of the Heath–Carter somatotype are very low (endomorphy: 2.67, mesomorphy: 2.12), the ectomorphic component (5.35) dominates her body shape; her somatotype reflects a

TABLE 2 Basic human characteristics of an endomorphic female, mesomorphic male, and ectomorphic female

Humans	Age (years)	Body mass (kg)	Body length (cm)	Basal metabolic flux density (Wm^{-2})	Walking energy flux density (Wm^{-2})	Total energy flux density (Wm^{-2})
Endomorphic female	24	132.5	168.5	43.6	144.8	188.5
Mesomorphic male	19	82	172.6	45.4	105.6	151
Ectomorphic female	19	46	166.1	41	80.7	121.2

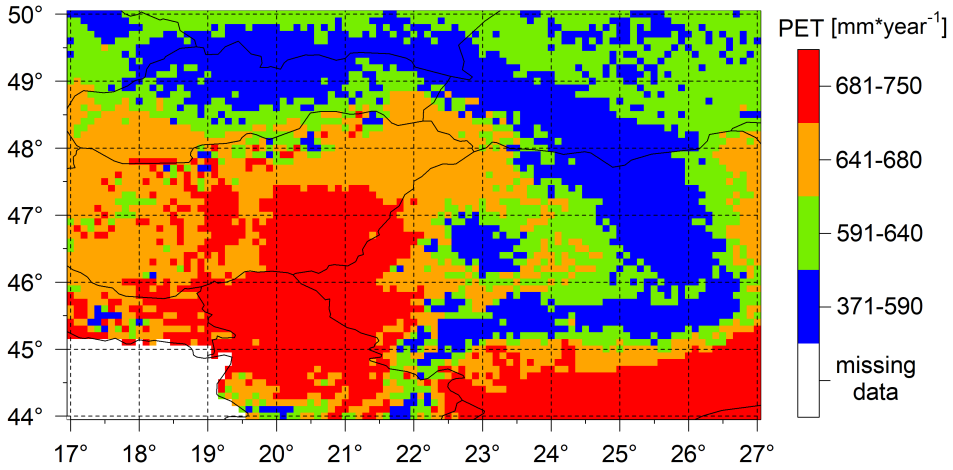

FIGURE 2 Area distribution of the annual sum of PET calculated using the Thornthwaite type (1948) formula in the CarpatClim dataset region for the period 1971–2000. Figures from 2 to 5 are constructed by the R programming language (R Core Team, 2019) [Colour figure can be viewed at wileyonlinelibrary.com]

TABLE 3 Somatotype component units of the three persons considered

	Somatotype components		
Humans	**Endomorphy**	**Mesomorphy**	**Ectomorphy**
Endomorphic female	9.24	7.42	0.50
Mesomorphic male	6.70	8.80	0.50
Ectomorphic female	2.67	2.12	5.35

linear body shape with very low fatness and musculoskeletal development.

3.3 | The thermal climate of the Carpathian region according to the r_{cl} model

The thermal climate of the region and the time period considered in terms of annual mean and annual fluctuation of clothing resistance values for an endomorphic, mesomorphic and ectomorphic human are presented in Figure 3.

Initially it is important to note that since the r_{cl} model is sensitive to human body somatotype variations, we avoid the use of arbitrary selected category boundaries for the r_{cl} and dr_{cl} values, which can lead to severely manipulated results. The application of the main percentiles (0th, 25th, 50th, 75th and 100th) of the r_{cl} and dr_{cl} values as category boundaries is an objective and reproducible categorisation method. At first glance, we can see that the area distribution structure of the r_{cl} and dr_{cl} fields is very similar for all three humans; the deviations are represented via their shifted r_{cl} and dr_{cl} values. The lowest r_{cl} and dr_{cl} values refer to endomorphic somatotype, the highest to ectomorphic somatotype. The area inhomogeneity of r_{cl} and dr_{cl} values is much larger in mountains than in lowlands. The hottest parts of the region are located in Banat, in these areas the r_{cl} values experienced by the ectomorphic somatotype are 0.59–0.96 [clo]. In this region, the area inhomogeneity is mostly caused by inhomogeneties in dr_{cl} fields. r_{cl} and dr_{cl} changes in the North Hungarian Mountains with respect to the lowlands can be unequivocally observed. Note how large the dr_{cl} values are on the Transylvanian Plateau, for the ectomorphic somatotype 2.26–3.05 [clo], and for the endomorphic somatotype 1.50–2.05 [clo]. dr_{cl} values decrease with increase of elevation, this can be observed going from the Wallachian Plain towards the Carpathians. So, for instance, for the mesomorphic somatotype dr_{cl} values decrease from 1.75–2.38 through 1.65–1.74 to 1.20–1.64 [clo]. In the same area the dr_{cl} values for ectomorphic somatotype decrease from 2.26–3.05 through 2.21–2.25 to 1.53–2.20 [clo] remaining above 2 [clo]. Similarly large dr_{cl} changes can be found on the Transylvanian Plateau.

Areas with large thermal contrast (adjacent pixels, or pixels close to each other, which have high and low r_{cl} and dr_{cl} values) are of special importance. Such areas can be observed around Mount Papuk, the Retezat Mountains and the Făgăras Mountains independently of somatotype. So, for instance, in the Făgăras Mountains r_{cl} changes from 0.17–0.48 to 0.67–1.26 [clo] for an endomorphic human and from 0.59–0.96 to 1.24–2.05 [clo] for an ectomorphic human. In summary: the thermal maps obtained possess great spatial heterogeneity, except in the central part of the Great Hungarian Plain. It is noteworthy that in this region a more detailed spatial pattern of any thermal indicator can be achieved; for example, for PET after its rescaling (Ács *et al.*, 2015).

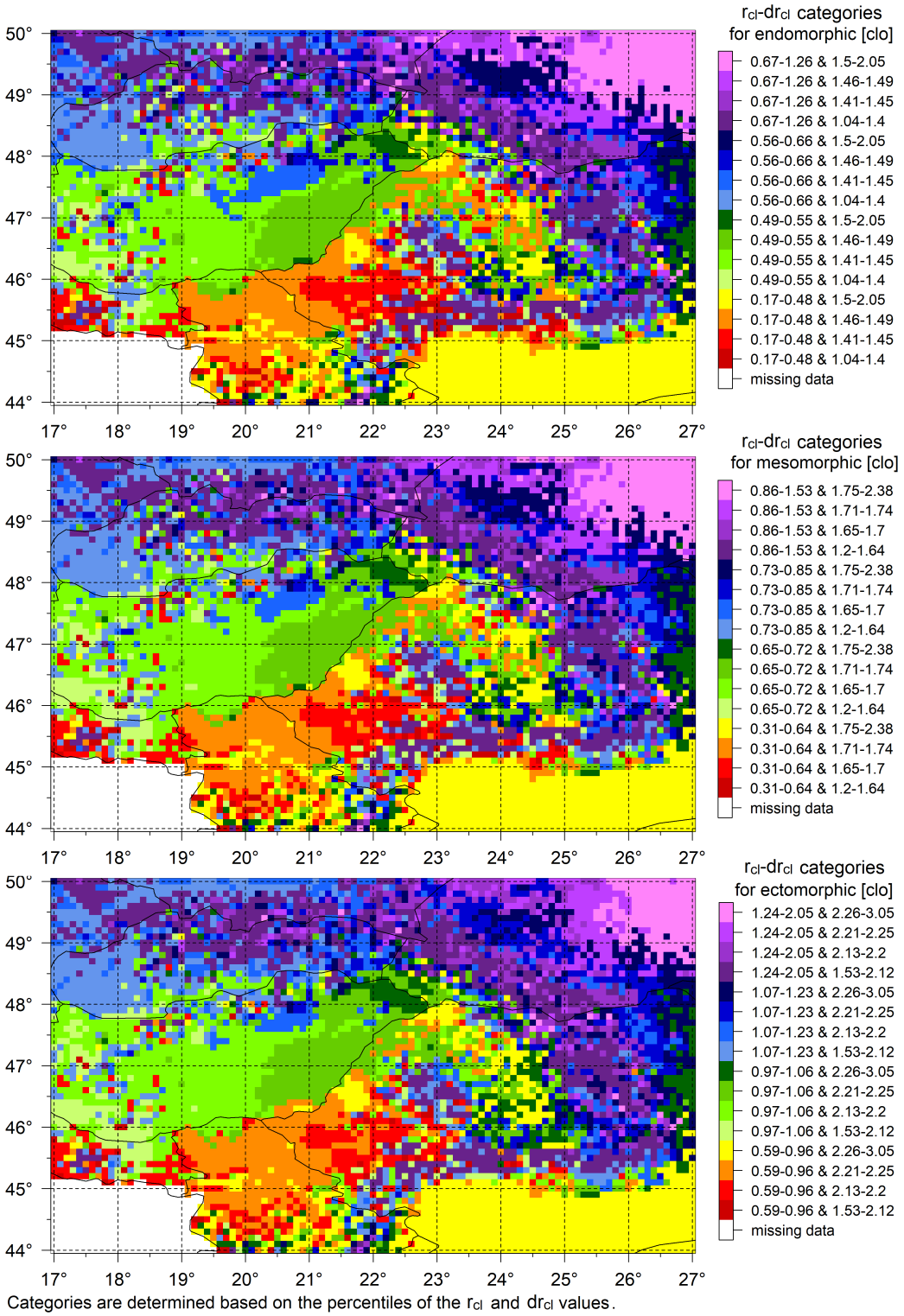

FIGURE 3 The area distribution of annual mean (r_{cl} in clo) and annual fluctuation (dr_{cl} in clo) clothing resistance values estimated by the model in the CarpatClim dataset region for the period 1971–2000 for an (a) endomorphic, (b) mesomorphic and (c) ectomorphic human. The annual fluctuation of clothing resistance is the difference of the maximum and the minimum monthly clothing resistance values. Figures 3 and 5 are created by using functions from packages maps (Brownrigg et al., 2018), fields (Nychka et al., 2017) and RColorBrewer (Neuwirth, 2014) [Colour figure can be viewed at wileyonlinelibrary.com]

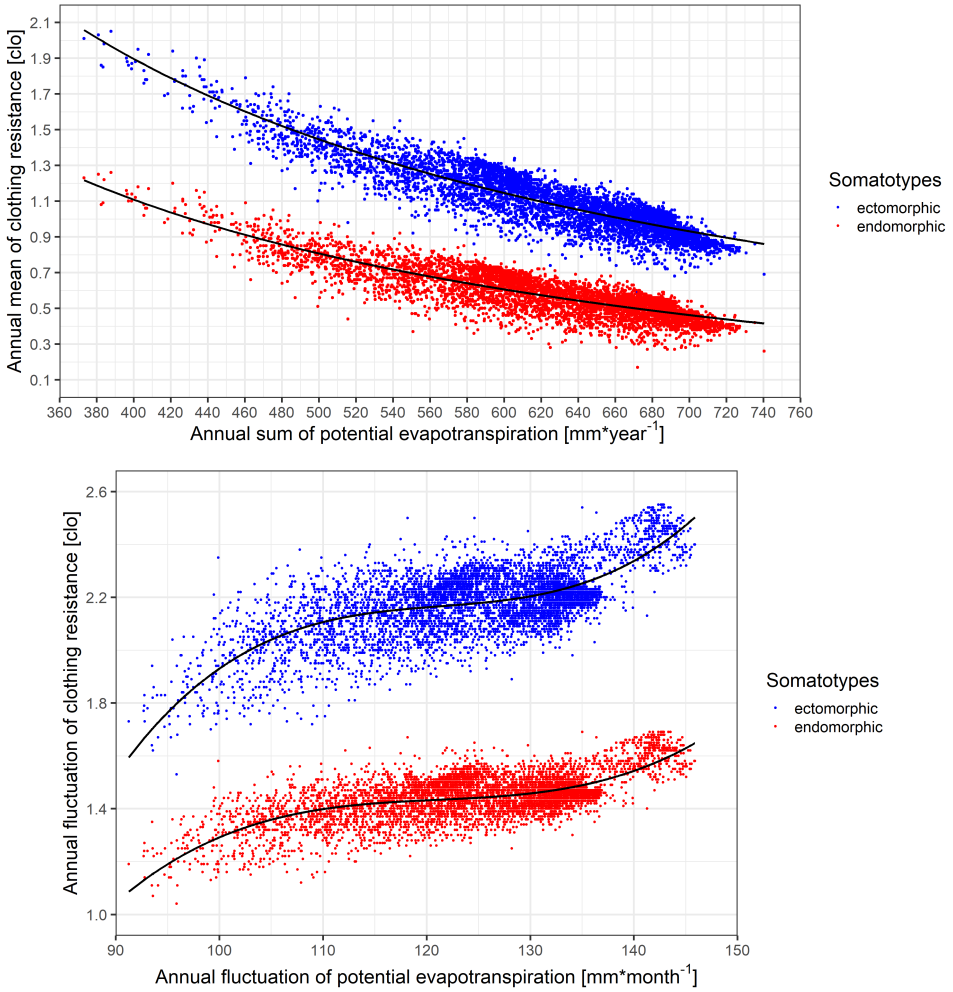

FIGURE 4 Scatter plot of (a) mean annual values of clothing resistance [clo] as a function of potential evapotranspiration ($mm \cdot year^{-1}$) and of (b) the annual fluctuation of clothing resistance [clo] as a function of annual fluctuation of potential evapotranspiration ($mm \cdot month^{-1}$) for the chosen ectomorphic and endomorphic humans and all climate types. The figure is constructed using the R functions from the ggplot2 package (Wickham, 2016) [Colour figure can be viewed at wileyonlinelibrary.com]

3.4 | Linking clothing resistance to potential evapotranspiration

The fields of mean annual r_{cl} and of annual sum of PET, as well as the fields of the annual fluctuation of r_{cl} and PET are constructed for the CarpatClim dataset region (about 6,000 grid points) and compared to each other. The results of the comparisons of the r_{cl} and PET fields and the dr_{cl} and dPET fields are presented in Figure 4.

Within the region PET ranges between 370 and 740 $mm \cdot year^{-1}$, the corresponding clothing resistance changes are between 1.2 and 0.3 [clo] for an endomorphic and 2.0–0.7 [clo] for an ectomorphic human, with clear separation between the somatotypes. The clothing resistance of an ectomorphic human r_{cl}^{ecto} is larger than the clothing resistance of an endomorphic human r_{cl}^{endo} since $M^{ecto} < M^{endo}$. The point cloud of a mesomorphic human is not presented to avoid congestion of points referring to three humans. A reciprocal model is fitted to the point clouds connecting r_{cl} and PET; the fitting coefficients and the R-squared values for all three somatotypes are given in Table 4. All regression coefficients can be considered as significant at a significance level of 0.1%. The distance between the two curves becomes slightly larger going from warmer (thermal type 'cool' [Feddema, 2005]) to colder (thermal type 'cold') PET values. The scatter of points linking dr_{cl} and dPET is much larger than the scatter of points linking r_{cl} and PET. dPET values vary between 90 and 145 ($mm \cdot month^{-1}$). dr_{cl} points ranges between 1.1 and 1.7 [clo] for an endomorphic and 1.6–2.5 [clo] for an ectomorphic human. dr_{cl} increases as dPET increases, but this increase is much slower in a range of dPET of 115–130 ($mm \cdot month^{-1}$). The point clouds connecting dr_{cl} and dPET are fitted by a third order regression polynomial; the fitting coefficients for all three somatotypes can be found in Table 5. The quality of the regression is better when regressing r_{cl} on PET than when regressing dr_{cl} on dPET. For both regression models, the quality of the regression is the best in the case of the ectomorphic human and the worst in the case of the endomorphic human.

TABLE 4 The fitting coefficients of the regression curve linking r_{cl} and PET for endomorphic, mesomorphic and ectomorphic humans

r_{cl} versus PET			
		Regression coefficients	
		Trend equation: $r_{cl} = a1 + (a2/PET)$	
Humans	***R*-squared (%)**	***a*1**	***a*2**
Endomorphic female	71	−0.40003	603.50673
Mesomorphic male	75	−0.38540	702.04940
Ectomorphic female	80	−0.35565	900.78154

Note: The regression curve equation is as follows: $r_{cl} = a1 + (a2/PET)$.

TABLE 5 The fitting coefficients of the regression curves linking dr_{cl} and dPET for endomorphic, mesomorphic and ectomorphic humans

dr_{cl} versus dPET					
Humans	*R*-squared (%)	Regression coefficients trend equation: $dr_{cl} = a1 \cdot dPET + a2 \cdot dPET^2 + a3 \cdot dPET^3 + b$			
		*a*1	*a*2	*a*3	*b*
Endomorphic female	43	0.48856	−0.00402	0.00001	−18.42959
Mesomorphic male	45	0.58694	−0.00483	0.00001	−22.21025
Ectomorphic female	48	0.78432	−0.00644	0.00002	−29.79622

Note: The regression curve equation is as follows: $dr_{cl} = a1 \cdot dPET + a2 \cdot dPET^2 + a3 \cdot dPET^3 + b$.

3.5 | The thermal climate of the Carpathian Basin according to regression curves connecting r_{cl} and PET and dr_{cl} and dPET

The r_{cl} and dr_{cl} thermal indicator maps obtained by the regression curves connecting r_{cl} and PET and dr_{cl} and dPET for endomorphic, mesomorphic and ectomorphic somatotypes are presented in Figure 5.

Inspecting Figure 5, we can hardly see differences in the spatial structure of r_{cl} and dr_{cl} values between different somatotypes. Some minor differences can be observed, for instance, in the Little-Hungarian Plain and in the southern parts of North Hungarian Mountains. The main characteristics of the region's thermal climate are well reproduced. So, for instance, the hottest areas are located in Banat, the thermal inhomogeneity in mountains is larger than in the lowland, the seasonal thermal fluctuation is less in the mountains than in the lowland and the areas with the largest thermal contrast are located around Mount Papuk, the Retezat Mountains and the Făgăras Mountains independently of somatotype. It is logical that the area inhomogeneity in Figure 5 (13 classes) is less than the area inhomogeneity in Figure 3 (16 classes). Note that Banat is cooler in Figure 5 than in Figure 3 independently of somatotype. So, for instance, in Figure 5, the range of r_{cl} for ectomorphic human is 0.86–0.97 [clo]; in Figure 3, the same r_{cl} is changing between 0.59 and 0.96 [clo]. In summary, thermal heterogeneity obtained by the models linking r_{cl} and PET and dr_{cl} and dPET is at least as well represented as the thermal heterogeneity obtained by Feddema's method, but its thermal heterogeneity is smaller than the thermal heterogeneity obtained by the clothing resistance model.

4 | DISCUSSION

The evolution of generic and human climate methods took place independently of each other. There have been only a few attempts at interconnecting them (e.g., Yang and Matzarakis, 2016; Potchter *et al.*, 2018; Ács *et al.*, 2020); in these studies, among the generic methods, the Köppen method was always used. In the work of Yang and Matzarakis (2016), the implementation of human thermal comfort information in Köppen–Geiger climate classification is done by estimating PET^h using the RayMan model (Matzarakis *et al.*, 2007) in 12 Chinese cities with 3-hr time resolution in the period 2000–2012. Human thermal comfort information is provided by determining frequencies of PET^h for PET^h <8°C (thermal sensation: cold, very cold), for PET^h >35°C (thermal sensation: hot, very hot) and for 8°C <PET^h <35°C (thermal sensation from cool to warm). Köppen's method is also used in the work of Potchter *et al.* (2018). This study reviewed the climatic variability of the neutral category

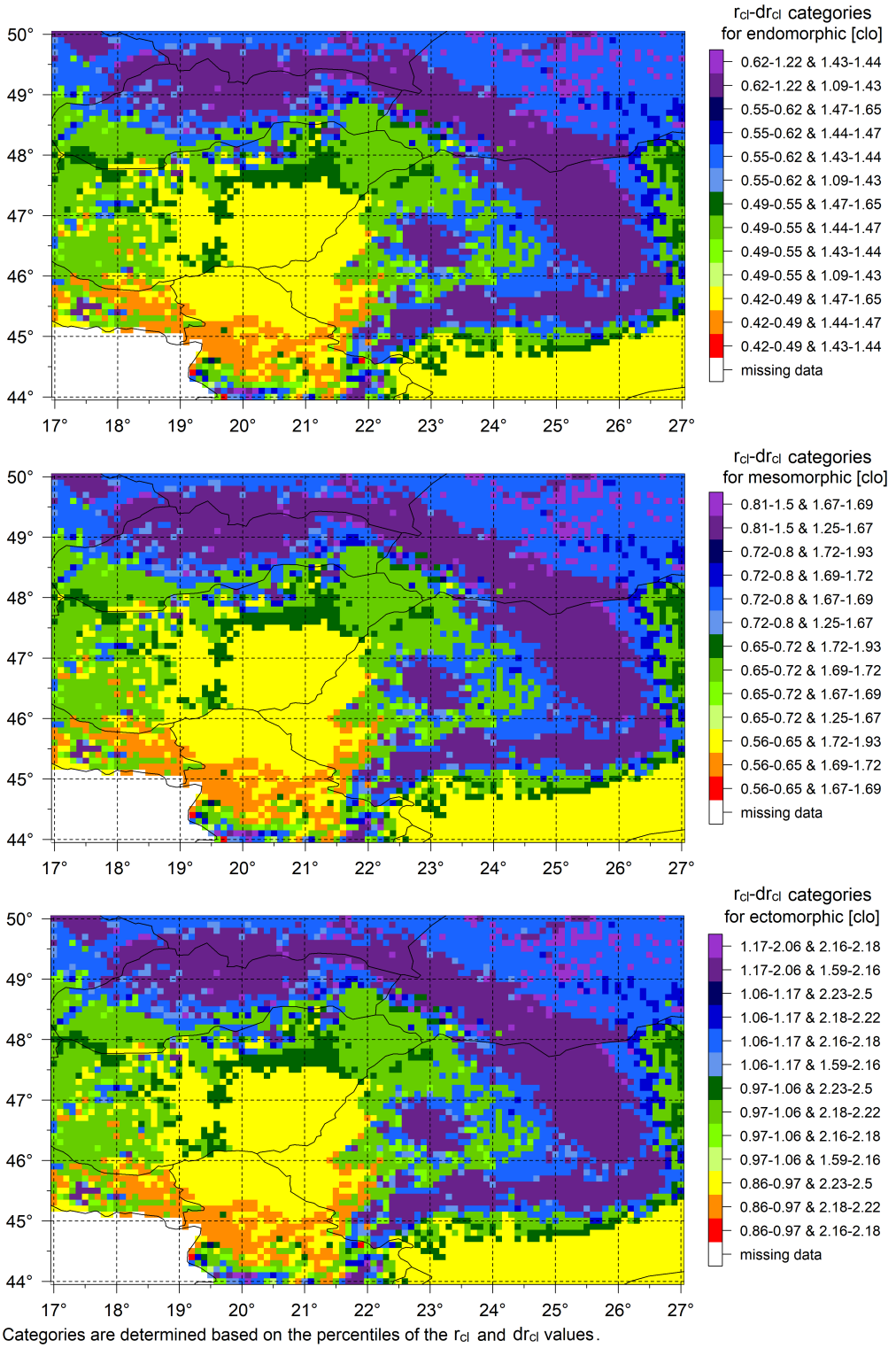

FIGURE 5 The area distribution of the annual mean (r_{cl} in clo) and annual fluctuation (dr_{cl} in clo) values of clothing resistance estimated using the regression curves connecting r_{cl} and PET and dr_{cl} and dPET in the CarpatClim dataset region for the period 1971–2000 for (a) an endomorphic, (b) mesomorphic and (c) ectomorphic human. The annual fluctuation of clothing resistance is the difference of the maximum and the minimum monthly clothing resistance values [Colour figure can be viewed at wileyonlinelibrary.com]

(no thermal stress) range of modified PET and the Universal Thermal Climate Index. The climate types are characterized by the Köppen method. Recently, Ács *et al.* (2020) have compared the area distribution of Köppen climate types and the clothing resistance parameter values in the Carpathian region. In this study, we have focused on potential evapotranspiration and clothing resistance with the aim to see (a) how they are capable of reproducing the Carpathian region's thermal climate characteristics and (b) whether there is the possibility to link them methodologically. We chose PET-based generic methods, since PET and human thermal indicators can be interconnected, if not otherwise then statistically. So far none of the human thermal climate

indicators have been linked to PET. The idea and the success of this linking are supported by fact that r_{cl} strongly depends on T_o (Equation 2), at the same time T_o and PET are similar quantities. They equally depend on radiation balance, air temperature and wind speed. Of course, there is no sense of interconnection of r_{cl} and PET in cold and very cold climates. In cold climates the interconnection of r_{cl} and T_a has to be preferred and this is a clear drawback of approaches based on interconnecting r_{cl} and PET. Our results suggest that the interconnection of r_{cl} and PET and dr_{cl} and dPET on the annual scale can be used in the Carpathian region. Having determined this link, we constructed the first hybrid models that methodologically interconnect human and descriptive climate model information. These statistical sub-modules can be used in Feddema's method for obtaining extra information regarding human thermal climates. Of course, both the r_{cl} and the PET models should remain as simple as possible. So, when simulating r_{cl} a one-node model (Katić *et al.*, 2016) is to be used; the use of two-node or multi-node models is not required since the treatment of skin temperature variation is not indispensable in climatological applications. PET, similarly to r_{cl}, should also be parameterised as simply as possible in climatological applications. Consequently, we preferred the air temperature based formula of McKenney and Rosenberg (1993).

Processing human data, an increase of the M of a walking human from ectomorphic through mesomorphic to endomorphic somatotype ($M^{ecto} < M^{meso} < M^{endo}$) is observed. The humans considered belong to completely different somatotypes, this is well illustrated by results presented in Table 3. The M-body shape relationship is not statistically proven, this is a task for the future. As a consequence, the strong dependence of r_{cl} on somatotype is noteworthy. This unique dependence in terms of human thermal sensation votes is not yet confirmed, this is also an important future task. Regarding the Carpathian region thermal climate characteristics, the following relationships can be highlighted: |(1) In terms of clothing resistance characteristics (annual mean of r_{cl} and annual fluctuation of r_{cl}) spatial heterogeneity is larger in mountainous areas than in lowlands. |(2) In terms of annual fluctuation of r_{cl} values, seasonal fluctuations are larger in lowlands than in mountainous areas. |(3) Areas with the largest thermal contrast are reproduced not only in terms of clothing resistance parameter but also in terms of annual sum of PET.

5 | CONCLUSIONS

The following main conclusions can be drawn: (1) On example of the Carpathian region, we showed that PET based generic methods can provide extra human thermal climate information by linking PET and the output of human thermal climate method, (2) extra human thermal climate information cannot be successfully served without having any information regarding the human body somatotype and (3) the Heath-Carter somatotype classification method seems to be a good tool for distinguishing inter-person or inter-human group variations in climatological applications.

ORCID

Ferenc Ács https://orcid.org/0000-0002-1611-6839

REFERENCES

Ács, F., Breuer, H. and Skarbit, N. (2015) Climate of Hungary in the twentieth century according to Feddema. *Theoretical and Applied Climatology*, 119, 161–169. https://doi.org/10.1007/s00704-014-1103-5.

Ács, F., Kristóf, E. and Zsákai, A. (2019) New clothing resistance scheme for estimating outdoor environmental thermal load. *Geographica Pannonica*, 23(4), 245–255. https://doi.org/10.5937/gp23-23717.

Ács, F., Zsákai, A., Kristóf, E., Szabó, A.I. and Breuer, H. (2020) Carparthian Basin climate according to Köppen and a clothing resistamce scheme. *Theoretical and Applied Climatology*, 141, 299–307. https://doi.org/10.1007/s00704-020-03199-z.

Auliciems, A. and de Freitas, C.R. (1976) Cold stress in Canada. A human climatic classification. *International Journal of Biometeorology*, 20(4), 287–294. https://doi.org/10.1111/j.1467-8470.1981.tb00373.x.

Auliciems, A. and Kalma, J.D. (1979) A climatic classification of human thermal stress in Australia. *Journal of Applied Meteorology*, 18, 616–626. https://doi.org/10.1175/1520-0450(1979)018<0616:ACCOHT>2.0.CO;2.

Bodzsár, É., Fehér, V.P., Vadászi, H. and Zsákai, A. (2016) A női nemi hormonok szintje és a testzsírosság kapcsolata pubertáskorú leányoknál (Sex hormonal levels and body fatness in pubertal girls). *Anthropológiai Közlemények*, 57, 51–60 (in Hungarian). ISSN: 0003-5440.

Bodzsár, É. and Zsákai, A. (2004) *Humánbiológia, gyakorlati kézikönyv (Humanbiology, practical manual)*. Budapest: ELTE Eötvös Kiadó, p. 300 ISBN 963 463 653 5.

Brownrigg, R., Minka, T. P., and Deckmyn, A.. (2018) maps: Draw Geographical Maps. R package version 3.3.0. Original S code by R.A. Becker, A.R. Wilks. https://CRAN.R-project.org/package=maps.

Campbell, G.S. and Norman, J.M. (1998) *An Introduction to Environmental Biophysics*, 2nd edition. New York, NY: Springer, p. 286.

Carter, J.E.L., Ross, W.D., Duquet, W. and Aubry, S.P. (1983) Advances in somatotype methodology and analysis. *Yearbook of Physical Anthropology*, 26, 193–213.

Carter, J.L. and Heath, B.H. (1990) *Somatotyping: Development and Applications*. Cambridge: Cambridge University Press, p. 503.

Cheval, S., Birsan, M.-V. and Dumitrescu, A. (2014) Climate variability in the Carpathian Mountains Region over 1961–2010. *Global and Planetary Change*, 118, 85–96.

de Freitas, C.R. (1979) Human climates of Northern China. *Atmospheric Environment*, 13, 71–77. https://doi.org/10.1016/0004-6981(79)90246-4.

Domonkos, P. (2013) Measuring performances of homogenization methods. *Időjárás*, 117, 91–112.

Dubois, D. and Dubois, E.F. (1915) The measurement of the surface area of man. *Archives of Internal Medicine*, 15, 868–881. https://doi.org/10.1001/archinte.1915.00070240077005.

Feddema, J.J. (2005) A revised thornthwaite-type global climate classification. *Physical Geography*, 26, 442–466. https://doi.org/10.2747/0272-3646.26.6.442.

Fiala, D., Havenith, G., Bröde, P., Kampmann, B. and Jendritzky, G. (2012) UTCI-Fiala multi-node model of human heat transfer and temperature regulation. *International Journal of Biometeorology*, 56(3), 429–441. https://doi.org/10.1007/s00484-011-0424-7.

Frankenfield, D., Roth-Yousey, L. and Compher, C. (2005) Comparison of predictive equations for resting metabolic rate in healthy nonobese and obese adults: a systematic review. *Journal of the American Dietetic Association*, 105, 775–789. https://doi.org/10.1016/j.jada.2005.02.005.

Gagge, A.P., Burton, A.C. and Bazett, H.C. (1941) A practical system of units for the description of the heat exchange of man with his environment. *Science*, 94, 428–430.

Gagge, A.P., Winslow, C.E.A. and Herrington, L.P. (1938) The influence of clothing on the physiological reactions of the human body to varying environmental temperatures. *American Journal of Physiology*, 124(1), 30–50. https://doi.org/10.1152/ajplegacy.1938.124.1.30.

Havenith, G., Fiala, D., Blazejczyk, K., Richards, M., Bröde, P., Holmér, I., Rintamaki, H., Benshabat, Y. and Jendritzky, G. (2012) The UTCI-clothing model. *International Journal of Biometeorology*, 56(3), 461–470. https://doi.org/10.1007/s00484-011-0451-4.

Jianbiao, L., Sun, G., McNulty, S. and Amatya, D.M. (2005) A comparison of six potential evapotranspiration methods for regional use in the southeastern United States. *The Journal of the American Water Resources Association (JAWRA)*, 41(3), 621–633. https://doi.org/10.1111/j.1752-1688.2005.tb03759.x.

Katić, K., Li, R. and Zeiler, W. (2016) Thermophysiological models and their applications: a review. *Building and Environment*, 106, 286–300. https://doi.org/10.1016/j.buildenv.2016.06.031.

Köppen, W. (1884) Die Wärmezonen der Erde, nach der Dauer der heissen, gemässigten, und kalten Zeitund nach der Wirkung der Wärme auf die organische Welt betrachtet. *Meteorologische Zeitschrift*, 1, 215–226.

Köppen, W. (1900) Versuch einer Klassifikation der Klimate, vorzugsweise nach ihren Beziehungen zur Pflanzenwelt. *Geographische Zeitschrift*, 6(593–611), 657–679.

Köppen, W. (1918) Klassifikation der Klimate nach Temperatur, Niederschlag und Jahresablauf. *Petermanns Geographische Mitteilung*, 64(193–203), 243–248.

Köppen, W. (1936) The geographic system of climates (original: das geographische system der Klimate). In: Köppen, W., Geiger, R. and Teil, C. (Eds.) *Handbuch der Klimatologie*. Berlin: Borntraeger, p. 44.

Kottek, M., Grieser, J., Beck, C., Rudolf, B. and Rubel, F. (2006) World map of the Köppen-Geiger classification updated. *Meteorologische Zeitschrift*, 15(3), 259–263. https://doi.org/10.1127/0941-2948/2006/0130.

Li, Z., Cao, L., Zhu, Y. and Yan, Z. (2016) Comparison of two homogenized datasets of daily maximum/mean/minimum temperature in China during 1960–2013. *Journal of Meteorological Research*, 30(1), 53–66. https://doi.org/10.1007/s13351-016-5054-x.

Lin, T.P. (2009) Thermal perception, adaptation and attendance in a public square in hot and humid regions. *Building and Environment*, 44(10), 2017–2026. https://doi.org/10.1016/jbuildenv.2009.02.004.

Matzarakis, A., Rutz, F. and Mayer, H. (2007) Modelling radiation fluxes in simple and complex environments – application of the RayMan model. *International Journal of Biometeorology*, 51, 323–334.

McKenney, M.S. and Rosenberg, N.J. (1993) Sensitivity of some potential evapotranspiration methods to climate change. *Agricultural and Forest Meteorology*, 64, 81–110. https://doi.org/10.1016/0168-1923(93)90095-Y.

Mifflin, M.D., St Jeor, S.T., Hill, L.A., Scott, B.J., Daugherty, S.A. and Koh, Y.O. (1990) A new predictive equation for resting energy expenditure in healthy individuals. *The American Journal of Clinical Nutrition*, 51, 241–247. https://doi.org/10.1093/ajcn/51.2.241.

Neuwirth E. (2014) RColorBrewer: ColorBrewer palettes. R package version 1.1–2. https://CRAN.R-project.org/package=RColorBrewer.

Nychka, D., Furrer, R., Paige, J., Sain, S.. (2017) fields: Tools for spatial data. R package version 9.9. https://cran.r-project.org/web/packages/fields/index.html. https://doi.org/10.5065/D6W957CT.

Potchter, O., Cohen, P., Lin, T.-P. and Matzarakis, A. (2018) Outdoor human thermal perception in various climates: a comprehensive review of approaches, methods and quantification. *Science of the Total Environment*, 631-632, 390–406. https://doi.org/10.1016/j.scitotenv.2018.02.276.

R Core Team (2019) R: A Language and Environment for Statistical Computing. R Foundation for Statistical Computing: Vienna, Austria. http://www.R-project.org/.

Rasol, D., Likso, T., and Milković J.. (2008). Homogenization of temperature time series in Croatia. *Proceedings of the Meeting of COST-ES0601 (HOME) Action Management Committee and Working Groups and the Sixth Seminar for Homogenization and Quality Control in Climatological Databases*, *Hungarian Meteorological Sevice*, *Budapest*, *Hungary*, 30 pp.

Robaa, S.M. and Hasanean, H.M. (2007) Human climates of Egypt. *International Journal of Climatology*, 27, 781–792.

Rubel, F. and Kottek, M. (2011) Comments on "The thermal zones of the Earth" by Wladimir Köppen (1884). *Meteorologische Zeitschrift*, 20(3), 361–365. https://doi.org/10.1127/0941-2948/2011/0285.

Spinoni, J., Antofie, T., Barbosa, P., Bihari, Z., Lakatos, M., Szalai, S., Szentimrey, T., and Vogt, J.. (2012) Comparing four drought indicators in the Carpathian Region on a 0.1x0.1 regular grid for 1961–2010. *Proceedings of 12th EMS–9th ECAC Conference*, *10–14 September*, *Lodz (PL)*.

Spinoni, J. and the CARPATCLIM project team . (2015) Climate of the Carpathian region in 1961–2010: climatologies and trends of 10 variables. *International Journal of Climatology*, 35, 1322–1341. https://doi.org/10.1002/joc.4059.39 authors

Szentimrey, T. (1999) Multiple analysis of series for homogenization (MASH). *Proceedings of the Second Seminar for Homogenisation of Surface Climatlogical Data*, *Budapest*, *Hungary*; WMO, WCDMP-No. 41, pp. 27–46.

Szentimrey, T. (2011) Manual of homogenization software MASHv3.03. Hungarian Meteorological Service, Budapest.

Thornthwaite, C.W. (1931) The climates of North America according to a new classification. *Geography Review*, 21, 633–655. https://doi.org/10.2307/209372.

Thornthwaite, C.W. (1948) An approach toward a rational classification of climate. *Geography Review*, 38, 55–94. https://doi.org/10.2307/210739.

Thornthwaite, C.W. and Mather, J.R. (1955) Water balance. In: *Climatology*, Vol. 8. Centerton, NJ: CW & Associates.

Utczás, K., Zsákai, A., Muzsnai, Á., Fehér, V.P. and Bodzsár, É. (2015) Radiológiai és ultrahangos módszerrel végzett csontéletkor-becslések összehasonlító elemzése 7–17 éveseknél (The analysis of bone age estimations performed by radiological and ultrasonic methods in children aged between 7–17 year). *Anthropológiai Közlemények*, 56, 129–138 (in Hungarian).

Weyand, P.G., Smith, B.R., Puyau, M.R. and Butte, N.F. (2010) The mass-specific energy cost of human walking is set by stature. *Journal of Experimental Biology*, 213, 3972–3979. https://doi.org/10.1242/jeb.048199.

Wickham, H. (2016) *ggplot2: Elegant Graphics for Data Analysis*. Berlin: Springer-Verlag.

Willmott, C.J. and Feddema, J.J. (1992) A more rational climatic moisture index. *The Professional Geographer*, 44, 84–88. https://doi.org/10.1111/j.0033-0124.1992.00084.x.

Winslow, C.-E.A., Herrington, L.P. and Gagge, A.P. (1937) *Physiological Reaction of the Human Body to Various Atmospheric Humidities. Contribution No. 16 from the John B.* New Haven: Pierce Laboratory of Hygiene, pp. 288–299.

Winslow, C.-E.A., Herrington, L.P. and Gagge, A.P. (1938) The relative influence of radiation and convection upon the temperature regulation of the clothed body. *American Journal of Physiology*, 124(1), 51–61.

Xu, C.-Y. and Singh, V.P. (2001) Evaluation and generalization of temperature-based methods for calculating evaporation. *Hydrological Processes*, 15, 305–319. https://doi.org/10.1002/hyp.119.

Yan, Y.Y. (2005) Human thermal climates in China. *Physical Geography*, 26(3), 163–176.

Yan, Y.Y. and Oliver, J.E. (1996) The Clo: a utilitarian unit to measure weather/climate comfort. *International Journal of Climatology*, 16, 1045–1056.

Yang, S.Q. and Matzarakis, A. (2016) Implementation of human thermal comfort information in Köppen-Geiger climate classification–the example of China. *International Journal of Biometeorology*, 60, 1801–1805. https://doi.org/10.1007/s00484-016-1155-6.

Yimer, S.M., Kumar, N., Bouanani, A., Tischbein, B. and Borgemeister, C. (2021) Homogenization of daily time series climatological data int he eastern Nile basin, Ethiopia. *Theoretical and Applied Climatology*, 143, 737–760. https://doi.org.10/1007/s00704-020-03407-w.

Zhen, L. and Zhong-Wei, Y. (2009) Homogenized daily mean/maximum/minimum temperature series for China from 1960-2008. *Atmospheric and Oceanic Science Letter*, 2(4), 237–243. https://doi.org/10.1080/16742834.2009.11446802.

Zsákai, A., Mascie-Taylor, N. and Bodzsár, É.B. (2015) Relationship between some indicators of reproductive history, body fatness and the menopausal transition in Hungarian women. *Journal of Physiological Anthropology*, 34(1), 35–42.

How to cite this article: Ács F, Zsákai A, Kristóf E, Szabó AI, Feddema J, Breuer H. Clothing resistance and potential evapotranspiration as thermal climate indicators—The example of the Carpathian region. *Int J Climatol*. 2021;41: 3107–3120. https://doi.org/10.1002/joc.7008